Journal of Alzheimer's Disease xx (2021) x–xx
DOI 10.3233/JAD-210378
IOS Press

High-Definition Transcranial Direct Current Stimulation Improves Delayed Memory in Alzheimer's Disease Patients: A Pilot Study Using Computational Modeling to Optimize Electrode Position

Ingrid Daae Rasmussen[a,b,*], Nya Mehnwolo Boayue[a], Matthias Mittner[a], Martin Bystad[a,b], Ole K. Grønli[b], Torgil Riise Vangberg[c,d], Gábor Csifcsák[a] and Per M. Aslaksen[a,e]
[a]*Department of Psychology, Research Group for Cognitive Neuroscience, Faculty of Health Sciences, UiT The Artic University of Norway, Tromsø, Norway*
[b]*Department of Geropsychiatry, University Hospital of North Norway, Norway*
[c]*Department of Clinical Medicine, University hospital of North Norway, Norway*
[d]*PET Center, University hospital of North Norway, Tromsø, Norway*
[e]*Department of Child and Adolescent Psychiatry, University Hospital of North Norway, Tromsø, Norway*

Handling Associate Editor: Jessica Peter

Accepted 28 June 2021
Pre-press 5 August 2021

Abstract.
Background: The optimal stimulation parameters when using transcranial direct current stimulation (tDCS) to improve memory performance in patients with Alzheimer's disease (AD) are lacking. In healthy individuals, inter-individual differences in brain anatomy significantly influence current distribution during tDCS, an effect that might be aggravated by variations in cortical atrophy in AD patients.
Objective: To measure the effect of individualized HD-tDCS in AD patients.
Methods: Nineteen AD patients were randomly assigned to receive active or sham high-definition tDCS (HD-tDCS). Computational modeling of the HD-tDCS-induced electric field in each patient's brain was analyzed based on magnetic resonance imaging (MRI) scans. The chosen montage provided the highest net anodal electric field in the left dorsolateral prefrontal cortex (DLPFC). An accelerated HD-tDCS design was conducted (2 mA for 3×20 min) on two separate days. Pre- and post-intervention cognitive tests and T1 and T2-weighted MRI and diffusion tensor imaging data at baseline were analyzed.
Results: Different montages were optimal for individual patients. The active HD-tDCS group improved significantly in delayed memory and MMSE performance compared to the sham group. Five participants in the active group had higher scores on delayed memory post HD-tDCS, four remained stable and one declined. The active HD-tDCS group had a significant positive correlation between fractional anisotropy in the anterior thalamic radiation and delayed memory score.
Conclusion: HD-tDCS significantly improved delayed memory in AD. Our study can be regarded as a proof-of-concept attempt to increase tDCS efficacy. The present findings should be confirmed in larger samples.

Keywords: Alzheimer's disease, computational modeling, NIBS, noninvasive brain stimulation, tDCS, transcranial direct current stimulation

*Correspondence to: Ingrid Daae Rasmussen, UiT The Arctic University of Norway, Huginbakken 32, N-9037, Norway. Tel.: +47 45251233; E-mail: ingrid.d.rasmussen@uit.no.

INTRODUCTION

While ultimately searching for a cure for Alzheimer's disease (AD), research on treatment options to slow cognitive decline plays an important role [1]. Transcranial direct current stimulation (tDCS) is a promising method for reducing memory impairment in AD [2]. During tDCS, two or more electrodes are placed on the scalp and deliver weak, typically 1–2 mA, current to the head, which induces electric fields in the cortex underneath the electrodes. Although promising, the results of applying tDCS to treat cognitive symptoms in AD are still inconsistent [3]. Even though key symptoms and patterns of brain atrophy related to AD are clearly defined, individual cases show great heterogeneity regarding the severity of symptoms, progression from early to severe stages, and the extent of brain degeneration [4]. All these factors can change the effectiveness of noninvasive brain stimulation on symptoms. Of note, however, are anatomical differences that may contribute strongly to variations in stimulation outcomes by influencing current distribution in the cortex [5, 6].

AD in its early stages is characterized by memory impairment [7], which can be measured with delayed memory tasks [8, 9]. Delayed memory refers to the ability to both recognize and recall information after a retention period. Although AD atrophy starts in the medial temporal lobe [10–12], frontal pathology is a key determinant of the clinical manifestations often reported by patients and their relatives [13]. In AD, neuroplasticity and excitability in the DLPFC are impaired [14]. Several tDCS studies have targeted the dorsolateral prefrontal cortex (DLPFC) in AD patients [15–18] since tDCS modulates neuronal activity and neuroplasticity by changing the excitability of stimulated brain areas [19].

In addition to gray matter atrophy, structural disconnections in AD have been demonstrated using diffusion tensor imaging (DTI), which enables the measurement of microstructural properties of the white matter. Several DTI studies have shown widespread white matter changes related to AD in temporal and parietal regions [20]. Studies have also revealed less fractional anisotropy (FA) and higher mean diffusivity (MD) in the cingulum bundle, the fornix and the splenium of the corpus callosum [21, 22]. In addition, AD patients have reduced FA in the anterior thalamic radiation (ATR) tract compared to both healthy controls and elderly patients with major depressive disorder [23]. The ATR tract connects the anterior and middle nuclear groups of the thalamus with the frontal lobes, and the DLPFC in particular [23, 24]. FA reduction in these pathways is correlated with cognitive decline [25]. Studies of white matter integrity and tDCS outcome in patients with aphasia, [26] healthy participants and stroke patients [27] report a positive relation between FA values and improvement on cognitive tasks after treatment. The association between white matter tract alterations in AD and tDCS treatment effects has not, to our knowledge, been investigated previously.

Computational modeling is an emerging method in the field of noninvasive brain stimulation and enables simulation of the distribution of electric currents across different brain areas and tissues [28]. The specific individual anatomy of the gyri and sulci, the amount and distribution of the cerebrospinal fluid (CSF), and the thickness of the scalp and skull are key variables that affect the pathway of tDCS currents [5, 6]. Supporting the role of CSF, Mahdavi and colleagues (2018) demonstrated that aging participants with gray matter reduction had lower current intensities in brain regions underneath the electrodes than younger participants without atrophy. A simulation study of two AD brains showed different effective stimulation sites in the cortex, even though electrode coordinates on the scalp were consistent [29]. To ensure that the target region of the cortex is affected by the tDCS-induced current, computational modeling may be especially important in AD studies, considering the strong heterogeneity in brain atrophy across patients [30–32].

Studies on AD to date have used conventional bipolar montages consisting of one anode electrode placed either over the left temporal cortex or over the left DLPFC, with the return electrode placed above the right hemisphere, often over the right DLPFC [2]. Modeling studies of conventional tDCS protocols demonstrate diffuse current flow between the electrodes, where the peak current density can be located between the two electrodes, rather than underneath [6, 31, 33, 34]. HD-tDCS increases focality, compared to conventional tDCS [33]. This method typically consists of smaller electrodes, in which one anode electrode is placed above the target region, surrounded by four return electrodes. This montage is also often referred to as a "4 × 1 montage" [6, 35].

Brain degeneration in AD is linked to both the progression of cognitive impairment [10] and to the alteration of tDCS-induced current propagation [29]. It is of clinical importance to study how gray matter atrophy and white matter alterations related to

AD impact the clinical effects of tDCS. A study by Kim and colleagues [36] in a nonclinical group revealed a positive correlation between current intensity in the DLPFC and performance on cognitive tasks after tDCS treatment. However, an analysis of tDCS-induced currents in the DLPFC has not been conducted in AD patients. It also remains elusive how anatomical properties are linked to performance on cognitive tests following tDCS in the AD population.

The aim of the present study was to investigate the effect of HD-tDCS on memory performance in patients with AD, with two main outcome measures: 1) cognitive test scores measured before and after HD-tDCS intervention and 2) MRI data investigating the relationship between inter-individual variability in brain anatomy and the effect of tDCS treatment. To optimize tDCS focality over the DLPFC, electrode placement was tailored to each individual patient. Computational modeling of HD-tDCS-induced electric fields was used to predict the current flow in each participant, aiding the selection of the electrode montage from a set of eight different possibilities that had a) the highest anodal stimulation in the DLPFC compared to other regions of the brain and b) of the montages that fulfilled rule a, the montage with the highest anodal current compared to the cathodal current in this region was chosen. Our main hypothesis was that participants receiving HD-tDCS would show better performance on delayed memory tasks after treatment than participants receiving sham stimulation. We also expected that individual anatomy would affect HD-tDCS treatment, with a negative correlation between improvement in delayed memory and white matter alterations, operationalized as reduced FA and increased MD. Cortical thickness, surface area and volume were hypothesized to have a positive correlation with memory improvement. Furthermore, we hypothesized that there would be a positive correlation between improvement in delayed memory after HD-tDCS and the tDCS-induced electric field in the left DLPFC.

MATERIALS AND METHODS

Participants

The study consisted of a double-blind, sham (placebo)-controlled, parallel-group trial, with an allocation ratio of 1:1. Participants had to fulfill the criteria for the diagnosis of probable AD according to the National Institute of Neurological and Communicative Disorders and Stroke Alzheimer Disease and Related Disorders Association (NINCDS-ADRDA [37, 38], section 4.2: "Probable Alzheimer's disease with increased level of certainty"). Further inclusion criteria were as follows: aged 60–85 years, a Mini-Mental Status Examination (MMSE) score of >17, and if medicated for AD (with memantine or cholinesterase inhibitors) the dose had to have been stable for >90 days. The exclusion criteria were depression or other psychiatric diagnoses present at enrollment, cancer, chronic obstructive pulmonary disease, metal in the body interfering with MRI, or severe sight- and/or hearing disabilities that would affect cognitive testing.

Participants were recruited from the Department of Geriatric Medicine at the University Hospital of North Norway (UNN), Tromsø. All participants signed written consent approved by The Regional Committees for Medical and Health Research Ethics (REK, project number 2017/794). This is a pilot study reporting the results of the first six HD-tDCS sessions of a more extensive study registered at ClinicalTrials.gov (Identifier: NCT03325205). MRI scans were performed at UNN. All other data were collected at UiT The Arctic University of Norway.

MRI acquisition

MRI data were acquired by a Siemens Skyra 3 T scanner located at UNN. T1-weighed images were acquired with a 3 D MPRAGE sequence with following parameters: TR/TE = 2300/ 2.96 ms, flip angle = 9°, matrix size = 256 × 256, 192 sagittal slices, and voxel size = 1 × 1 × 1 mm. T2-weighed images were acquired with a 3 D turbo spin echo sequence with the following parameters: TR/TE = 14,404/93 ms, flip angle = 111°, no fat suppression, matrix size = 256 × 256, 192 sagittal slices, voxel size = 1 × 1 × 1 mm. DTI was acquired with: TR/TE = 10,700/80 milliseconds, b-value = 1000 s/mm^2, 30 gradient directions, matrix size 112 × 112, with 70 axial slices 2 mm thick, voxel size = 2 × 2 × 2 mm, with parallel acceleration factor 2. Total scan time was 24 min.

Creation of head models and computational modeling

Head models creation and simulation of the tDCS-induced electric field (E-field) were based on the pre-released version of SimNIBS 2.1 (http://www.simnibs.org/) [39]. The E-field was simulated for eight different 4 × 1 montages centered

Table 1
Electrode positions for the eight HD-tDCS montages used for simulation in SimNIBS

Anode	Cathodes
F3	F7, C3, Fz, and Fp1
F5	F9, C5, F1, and Fp1
FFC5h	AF3, F7, FTT7h, and FCC3h
FC3	FT7, CP3, FCz, and AF3
FFC3h	AFF5h, FCC5h, FCC1h, and AFF1h
F1	F5, C1, F2, and Fp1
AF3	AF7, FFC5h, Fz, and Fpz
AFF5h	F9, FC3, AFF1h, and Fp1

Electrode labels are based on the extended 10/20 EEG- system.

over the DLPFC for each brain (Table 1). Calculations of the normal component of the E-field were based on the finite element method (FEM) [40]. The normal component is oriented perpendicular to the cortical surface, with the current either flowing inward or outward. Current entering the cortex is commonly associated with increased neural excitability ("anodal effect", positive values of the normal component), whereas current leaving the gray matter towards the CSF is inhibitory in nature ("cathodal effect", negative values of the normal E-field) [41]. Detailed head models were created based on T1 and T2 MRI images, consisting of five different tissue types: skin, skull, gray matter, white matter, and CSF (Fig. 1). Conductivity values for the different tissue types were based on default settings in SimNIBS (Supplementary Table 1). The DLPFC was located in each brain according to the Ranta atlas [42, 43]. The electrode montage was chosen based on two rules. Rule 1 was that the highest value of anodal current had to be in the left DLPFC compared to other regions in the frontal cortex. For the montages that fulfilled rule 1, rule 2

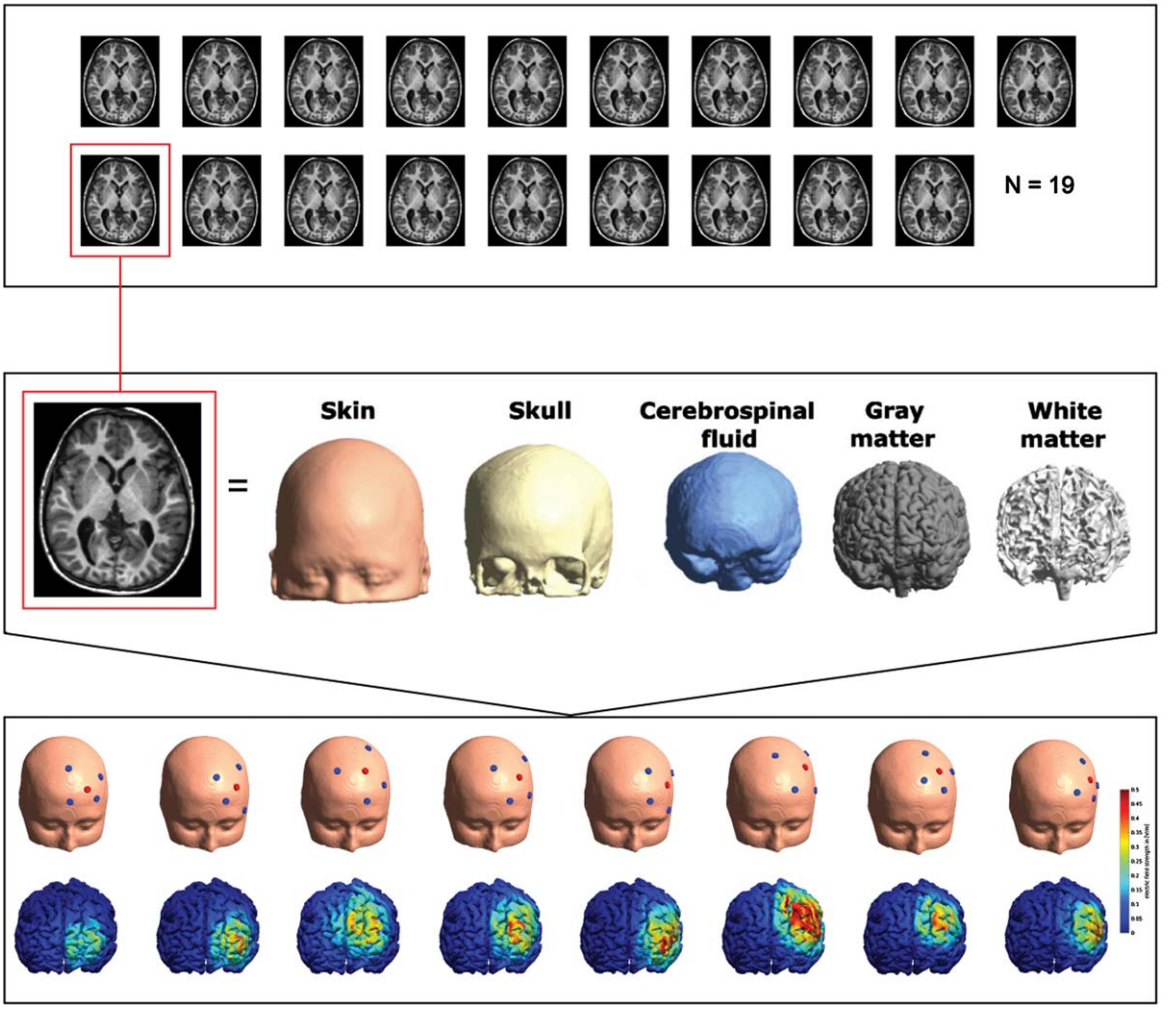

Fig. 1. Computational modeling workflow. Each patient's MRI (top panel) was used to create detailed anatomically realistic head models (middle panel). For each of these head models, we simulated eight different electrode placements centered over the DLPFC (bottom panel).

was applied, which was that the montage with the highest difference between anodal minus cathodal E-field in the left DLPFC was chosen. This second rule was designed to prevent strong cathodal currents in the target area, which are associated with neural inhibition. Therefore, this measure of the difference between anodal and cathodal E-fields can be regarded as the "net" maximal anodal E-field in the target area.

All electrodes were round-shaped, with a diameter of 12 mm and thickness of 1 mm plus a gel layer of 2.5 mm. Current intensity for the anodal electrode was set to 2 mA, with each of the 4 cathodes receiving a current intensity of 0.5 mA. Individual placement of tDCS electrodes was achieved by first manually defining four reference points (nasion, inion, left and right pre-auricular points), and using these as inputs to an adapted version of a published script [44].

Group allocation: Real HD-tDCS and sham HD-tDCS

Block randomization was generated by a computer randomization list (Randomizer.gov). The list was prepared by an investigator with no clinical involvement in the trial. The allocation rate was 1:1 using block sizes of 10. Labels depicting anodal tDCS ("1") and sham tDCS ("2") were placed in sealed envelopes with serial numbers written on the envelope according to the randomization list. The envelopes were shuffled, and the participants received the envelope at the top of the pile when enrolled in the study. The tDCS device was set to double-blind mode.

tDCS

Active or sham HD-tDCS was applied over the DLPFC via five surface-based round electrodes (12 mm in diameter) using a CE mark-approved Starstim® tDCS system from Neuroelectrics. There was a single anode electrode in the middle (2 mA) surrounded by four cathode electrodes (0.5 mA each). The montage over the DLPFC was optimized for each participant based on the results from computational modeling (see "Creation of head models and computational modeling"). The electrodes were fixed to the head using the Starstim cap for the F3 montage and a 128 channel EEG cap for the other montages. For the HD-tDCS group, the current was ramped up to 2 mA over a duration of 30 s and remained at this strength for 19 min before it was ramped down to 0 mA over the last 30 s. For the sham condition, the current was ramped up to 2 mA over the first 30 s and then ramped down again to 0 mA during the next 30 s. The same procedure was performed after 18 min. This sham procedure does not give a significant dose of tDCS, but makes the patients feel both the ramp up and ramp down sensation of tDCS to increase blinding. A total of six sessions were applied over two days, with one or two days of rest in between. Three HD-tDCS sessions were given each day with an "accelerated tDCS design" of 20 min of HD-tDCS – 15 min of rest – 20 min of HD-tDCS – 15 min of rest – 20 min of HD-tDCS. All participants received a local anesthetic (EMLA) cream applied to the locations at the scalp where the electrodes would be placed 30 min before the stimulation, for reducing both itching and discomfort in the HD-tDCS group and to facilitate higher blinding efficiency between the two groups. During the stimulation- sessions the patients were seated comfortable in a chair, resting. The "offline" design was chosen based on previous reviews showing that offline tDCS was found to be more effective than "online" designs for older adults [45]. The design was also chosen to make the tDCS procedure less overwhelming for the AD patients that suffer from reduced cognitive capacity with increased risk of tiredness. To make the test situation as similar as possible between pre- and post-testing and to minimize test- fatigue in AD patients, post-tests were administered with a two-day delay after the last HD-tDCS session. An additional rationale for the two-day delay was to measure whether multiple sessions of tDCS in an accelerated design gave effects useful for the patients in their daily living, based on LTP effects, rather than solely acute effects [46].

The participants visited the university five times for different procedures, including screening and pretesting, six active or sham sessions of HD-tDCS and post-test (see Fig. 2).

Neuropsychological assessment

The primary outcome measures were immediate and delayed verbal memory, based on tests from

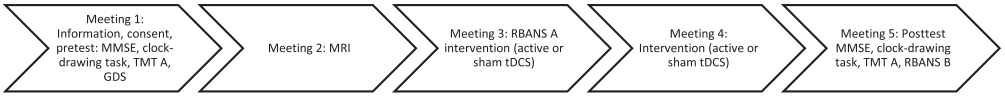

Fig. 2. Procedure for testing and treatment.

the Repeatable Battery for the Assessment of Neuropsychological Status (RBANS). RBANS is a standardized neuropsychological test battery used in both basic research and clinical assessment [47–49]. The test shows high specificity (82%) and sensitivity (98%) for the detection of AD [50]. Immediate memory consists of a 10-item list that is repeated and that the participant is to immediately recall four times and a story that is repeated and that the participant is to immediately recall two times. Delayed memory consists of both verbal and visual memory tasks. After approximately 20 min, the 10-item list was used to test recall and recognition, whereas a story was used to test recall. In addition, there is a visual recall test of a complex figure. RBANS consists of two parallel versions (A and B), with different wordlists and stories to reduce test-retest effects. Reliability coefficients are between 0.81 and 0.94 for the population between 60 and 89 years of age [47]. Secondary outcome measures consisted of global cognitive function using the RBANS battery, covering five domains: immediate verbal memory, visuospatial/constructional, language, attention, and delayed visual and verbal memory. Screening tests for dementia were also part of the secondary outcomes, consisting of MMSE [51], clock drawing test [52], and Trail Making Test part A [53].

MRI analysis

Volume, surface area and thickness values were provided by FreeSurfer version 6.0 software [54] with the recon-all processing pipeline. This pipeline includes motion correction, normalization to Talairach space, intensity bias correction, skull stripping, surface registration and segmentation. FreeSurfer segmentation outputs were visually inspected in Freesurfers visualization application *Free View* for severe errors as recommended in the FreeSurfer documentation (e.g., skull strip errors, segmentation errors, and pial surface misplacement) and no severe errors were found. Thus, no manual correction was performed on the segmentation outputs. To calculate cortical thickness, FreeSurfer use the algorithm of mean distance between vertices of a corrected, triangulated white matter surface and the pial surface [55]. See Fischl and colleagues [56, 57] for a full description of the FreeSurfer processing steps of parcellation and segmentation. The hippocampal volume and the parcellated thickness of the entorhinal cortex were analyzed since they are hallmark structures of AD atrophy [10]. Based on the modeling studies of Miranda [28] showing altered tDCS-current distribution due to gray matter atrophy, analysis of total gray matter volume was also included in the measurements in FreeSurfer.

Statistical analyses of cortical thickness and surface area were performed within the software package Permutation Analysis of Linear Models (PALM) [58]. Mris_preproc was used for resampling the individual surfaces to an average surface to accommodate statistical analysis in FS 6.0. The design matrixes for the permutation analyses consisted of score changes on the delayed memory test and in age. Both covariates were mean centered before the analyses. Permutation analyses were performed with 5000 iterations, and threshold-free cluster enhancement (TFCE) [59] was used for correction for multiple comparisons [60]. A familywise error rate-corrected $p < 0.05$ was considered significant.

The major white matter pathways were automatically reconstructed with TRActs Constrained by UnderLying Anatomy (TRACULA) [61]. TRACULA relies on the underlying anatomy from the cortical parcellation and subcortical segmentation accomplished using FreeSurfer. The trac-all script was run that involved a) preprocessing of the DWI (correction for motion and eddy currents), b) registration of the individual DW and anatomical images to the common (atlas) space, c) reconstruction of white matter tracts from the template using a deterministic fiber tracking algorithm and d) extraction of statistics on standard diffusion measures (FA and MD) for each reconstructed pathway. Labeling of white matter tracts was based on an established protocol [62]. Since the tDCS current was delivered to the left DLPFC, the following tracts were analyzed: left anterior thalamic radiation (lATR), left cingulum cingular bundle (lCCG), and forceps minor (FMIN). It

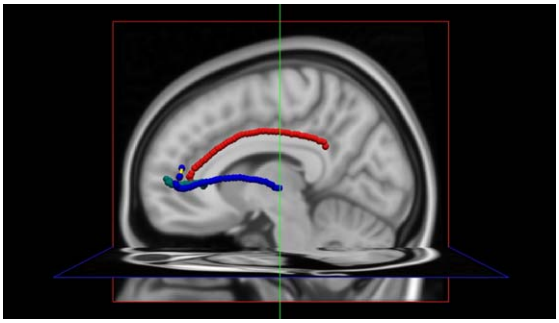

Fig. 3. White matter tracts. Green: Forceps minor. Blue: left hemisphere Anterior Thalamic Radiation. Red: left hemisphere cingulum cingular bundle.

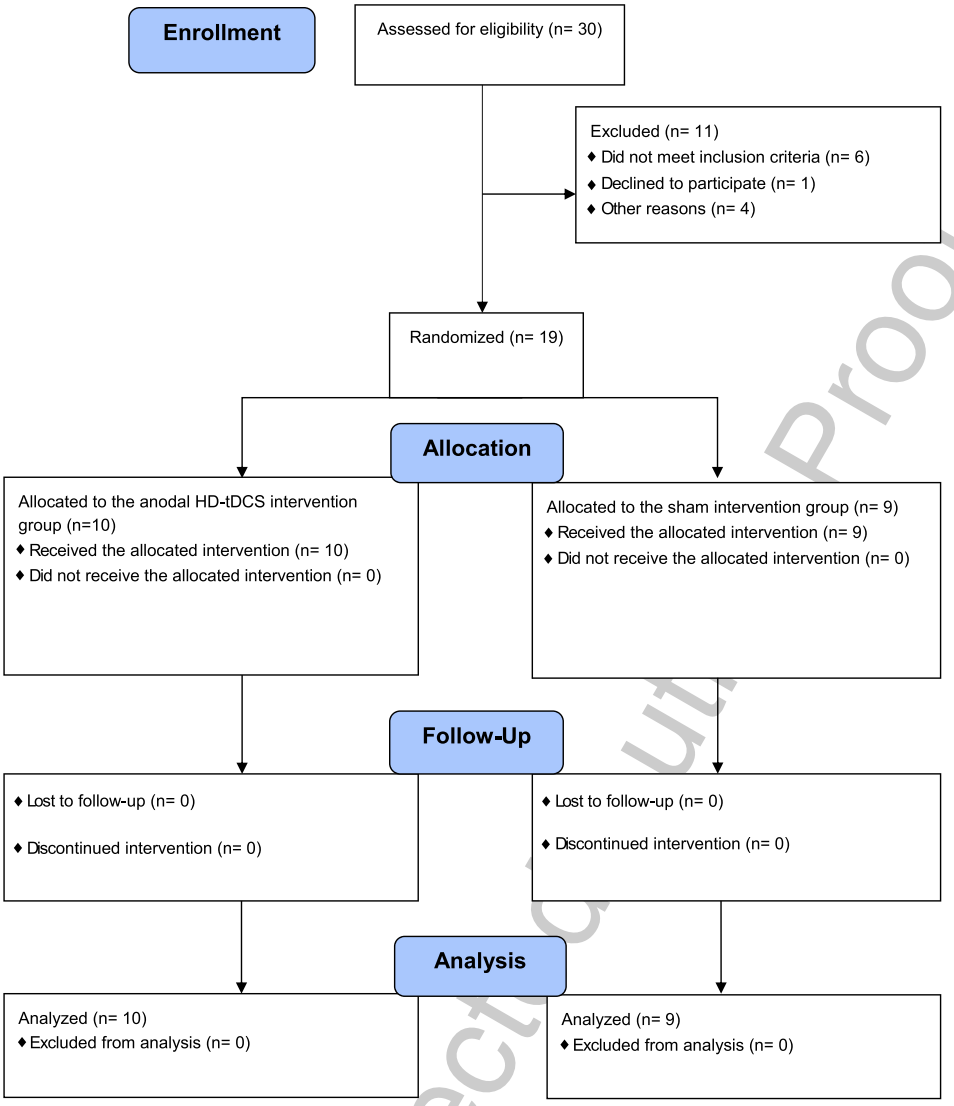

Fig. 4. CONSORT flow diagram showing participant flow through each stage of the trial.

was assumed that these tracts would be stimulated by the tDCS current due to their connections and/or closeness to the DLFPC (Fig. 3). High FA values represent higher structural connectivity between nodes in a network. Individual differences in white matter (variations in structural connectivity) may influence the behavioral response to stimulation [27].

Statistical analyses

The demographic and clinical characteristics of the participants are described with means and standard deviations (SDs). Independent *t*-tests were used to compare the demographic and baseline data. Generalized linear models were used to test the difference between groups from baseline to post-test on the outcome variables. The probability distribution used in the generalized regression models were normal distributions with identity links. The change scores (baseline – post-test) of the variables Delayed memory, Immediate memory, MMS, TMT, Clock Drawing Test, Verbal Performance, Visuospatial Performance, Attention, and RBANS total were used as dependent variables in separate analyses. Due to the small sample size, only group, baseline performance of the dependent variable, sex, and age of the participants were included as factors and covariates.

The HD-tDCS group was further divided into two subgroups based on their performance on the cognitive tests: a positive effect (PE) group, defined by a

positive change in score on the delayed memory test, and a no effect (NE) group, defined by no change in score/negative change in score. An independent *t*-test was performed to assess whether there was a difference in E-field intensity in the left DLPFC between the PE and NE groups. To provide additional information, effect sizes (Hedges' g) were calculated for the *t*-tests. Values ≤ 0.49 indicated small effects, $0.50 \leq g \leq 0.79$ indicated medium effects, and $g \geq 0.80$ indicated large effects. The results were expressed as the mean $\pm$ SD. Data were analyzed with SPSS version 26 (http://www.spss.com). p values below 0.05 were considered statistically significant.

RESULTS

Data collection for this study took place from July 2017 to March 2020. Thirty (N = 30) participants with a mean age of 78.80 ± 7.42 years (22 females) consented to participate. Six participants scored lower than 17 on the MMSE screening test and were excluded from the study. One participant decided to withdraw after Meeting 1 (due to worsening of the disease). Three participants could not complete the study due to the COVID-19 lockdown. Twenty participants underwent MRI scans. One participant was excluded due to poor MRI scan quality. A flow diagram is shown in Fig. 4. All analyses are based on a final sample of nineteen participants (N = 19), with an age range from 61 to 83 years and a mean age of 72.58 ± 7.19 years (14 females). No adverse effects were reported or observed during the intervention.

Baseline characteristics

Table 2 shows the baseline characteristics of the two groups. There was a significant difference in the delayed memory scores at baseline (HD-tDCS group: M = 14.00, SD = 2.87, sham group: M = 22.67, SD = 9.79; $t(17) = -2.68$, $p = 0.016$). The maximum score possible on the delayed memory tasks was 62.

Optimal electrode montage

Of the eight different montages that were simulated over the left DLPFC, four were selected for at least one of the participants (Table 3). See Fig. 5 for an example of a chosen montage over the DLPFC.

Effect of HD-tDCS on cognitive performance

A Shapiro-Wilk test ($p > 0.05$) and a visual inspection of the participants' histograms, normal Q-Q plots, and box plots showed that all RBANS subscores and the RBANS total score for the two groups were not significantly different from normal distributions. For the screening tests (MMSE, Clock Drawing Test, and TMT), however, data from the sham group were not normally distributed. In the HD-tDCS group, data for all screening tests except the clock-drawing test were normally distributed.

The generalized linear model showed that delayed memory change scores were different between the HD-tDCS group and the sham group shown by the main effect of group (B = 3.13, SE = 1.51, Wald χ^2 (1) = 4.26, $p = 0.039$) with higher change in the HD-tDCS group compared to the sham group. None of the other included covariates (baseline memory performance, age, and sex) reached significance (all

Table 2
Baseline characteristics

Measures *Demographics*	Total (Mean $\pm$ *SD*)	HD-tDCS group (Mean $\pm$ *SD*)	Sham group (Mean $\pm$ *SD*)	*p*
Number	19	10	9	
Age		69.20 ± 5.92	76.33 ± 6.84	0.026*
Sex (Females:Males)	14:5	9:1	5:4	0.098
Test scores (Maximal scores)				
RBANS delayed memory *(92)*	18.11 ± 8.15	14.00 ± 2.87	22.67 ± 9.79	0.016*
RBANS immediate memory *(64)*	24.84 ± 10.63	23.00 ± 10.92	26.89 ± 10.53	0.442
RBANS visuospatial *(40)*	26.79 ± 8.75	25.80 ± 8.39	27.89 ± 9.52	0.618
RBANS attention *(92)*	26.42 ± 12.74	26.90 ± 9.12	25.89 ± 16.47	0.869
RBANS language *(49)*	17.10 ± 6.71	18.30 ± 8.11	15.78 ± 4.84	0.429
RBANS total *(634)*	297.42 ± 79.78	*288.40 ± 70.81*	*307.44 ± 92.01*	*0.618*
MMSE *(30)*	21.26 ± 4.09	20.00 ± 3.40	22.67 ± 4.53	0.162
Clock-drawing test *(5)*	3.63 ± 1.54	3.30 ± 1.70	4.00 ± 1.32	0.335
TMT A *(240)*	75.11 ± 30.05	65.60 ± 10.10	85.67 ± 40.97	0.151

MMSE, Mini-Mental Status Examination; TMT A, Trail Making Task A. RBANS raw scores. *Indicates $p < 0.05$.

Table 3
Overview of all simulated stimulation montages and how often they were chosen in the HD-tDCS and sham groups

Anode	Cathodes	Chosen montage	
		HD-tDCS group	Sham group
F3	F7, C3, Fz, and Fp1	5	5
F5	F9, C5, F1, and Fp1		–
FFC5h	AF3, F7, FTT7h, and FCC3h	–	–
FC3	FT7, CP3, FCz, and AF3	–	–
FFC3h	AFF5h, FCC5h, FCC1h, and AFF1h	1	–
F1	F5, C1, F2, and Fp1	–	–
AF3	AF7, FFC5h, Fz, and Fpz	1	–
AFF5h	F9, FC3, AFF1h, and Fp1	3	4

Electrode labels are based on the extended 10/20 EEG- system.

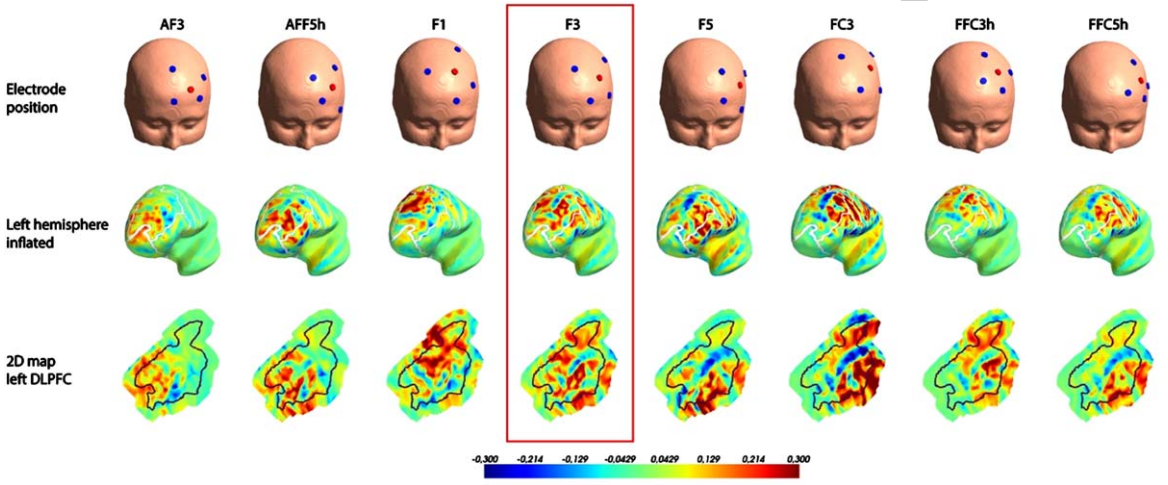

Fig. 5. Selection of the optimal electrode montage for the DLPFC in one participant. Selected montage is based on the net maximal anodal E-field in the left DLPFC. Row 1: electrode placement on the head (with the label of the anode highlighted in red). Row 2: Inflated brains showing the left hemisphere. Row 3: 2D map of the left DLPFC, with the magnitude of the normal component of the electric field depicted in a polarity-specific way (anodal E-field: hot colors; cathodal E-field: cold colors).

ps > 0.39). MMSE performance improved in the HD-tDCS group compared to the sham group (B = 2.78, SE = 1.12, Wald χ^2 (1) = 6.13, $p = 0.013$), and the effect of Age on the change score on MMSE was significant (B = –0.16, SE = 0.08, Wald χ^2 (1) = 2.49, $p = 0.041$) showing that lower age was associated with better MMSE performance. There were no other significant group effects for the other outcome variables, see Supplementary Table 2.

E-field in the left DLPFC and score changes on the delayed memory subtest

Pearson's correlation analysis indicated a non-significant positive correlation between the score change on the delayed memory subtest in the HD-tDCS group and the net maximal anodal E-field in the DLPFC (r(8) = 0.34, $p = 0.34$). An independent *t*-test showed no significant difference in the net anodal E-field in the target region between the participants who had improved performance on delayed memory after HD-tDCS treatment (M = 0.07 V/m, SD = 0.03) and the participants who did not show improved performance on memory tasks after HD-tDCS treatment (M = 0.05 V/m, SD = 0.003); t(8) = 1.26, $p = 0.242$. However, the effect size was $g = 0.78$, indicating that participants in the HD-tDCS with improved memory scores had a moderately higher mean net anodal E-field in the DLPFC than participants who did not improve their delayed memory performance after HD-tDCS. Figure 6 shows the score change on the

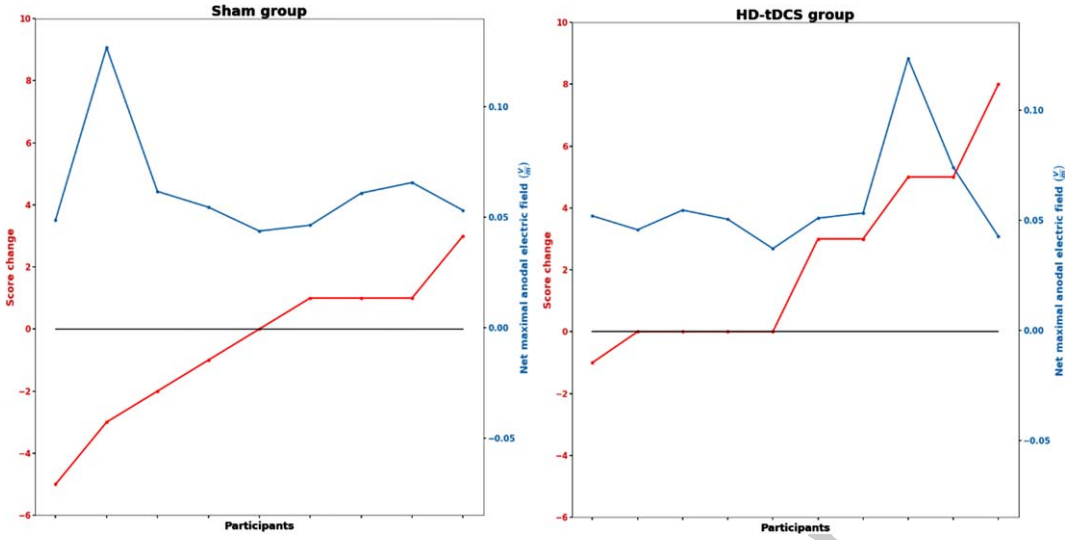

Fig. 6. Score changes in the delayed memory subtest and net anodal E-field in the left DLPFC. Score changes in the delayed memory subtest (red) and net anodal E-field in the left DLPFC (blue) in the sham and HD-tDCS groups. Dots on the same vertical line represent a participant. In both groups, patients are ordered according to the magnitude of the increase in the delayed memory subtest score.

delayed memory subtest and the maximal anodal E-field value in the DLPFC for each participant.

Relationship between score changes and brain volume, cortical thickness, and cortical surface area

Correlation analysis of MRI data collected at baseline (total gray matter volume, volume of the left and right hippocampus, and cortical thickness of the left and right entorhinal cortex) and score changes on the delayed memory subtest showed no significant results (Supplementary Tables 3 and 4). Permutation analyses showed no statistically significant differences in cortical thickness or surface area between the HD-tDCS and sham groups at baseline. There was a tendency towards an association between cortical thickness and score changes on the delayed memory subtest, whereas participants in the HD-tDCS group with a thicker cortex in regions in the left hemisphere had higher score changes on the delayed memory tasks (Fig. 7). The results were non-significant. These associations were not found in the right hemisphere in the HD-tDCS group. No association was found in the sham group regarding thickness/surface area and score changes for delayed memory.

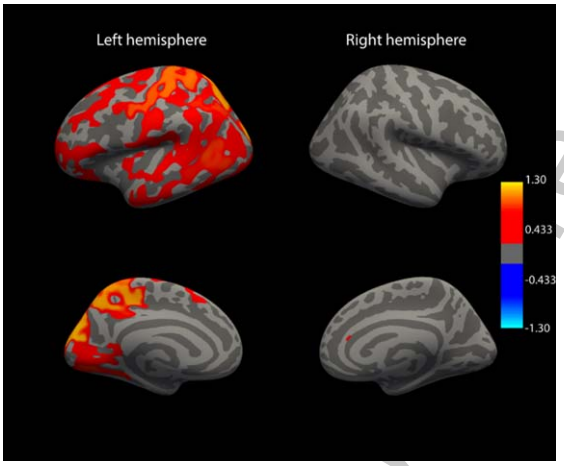

Fig. 7. PALM analysis of cortical thickness in the left hemisphere and score changes on the delayed memory test. Analysis showing a tendency towards an association between cortical thickness and score change on delayed memory in the HD-tDCS group. This association was not statistically significant. Color bars indicate –log10(p) thresholds. Values of 1.3 imply a relation that is statistically significant at $p < 0.05$. The max value in the plot was 1.12, indicating a p value of 0.075.

Correlation between memory performance and DTI parameters

FA and MD were measured in the lATR, lCCB, and FMIN. Analysis was based on 16 participants due to low quality MRI to complete DTI analysis for three of the participants (HD-tDCS group = 9, sham group = 7). *T*-tests showed no significant group difference in DTI measures between the active and sham groups at baseline (Fig. 8). Correlation analysis (Table 4) showed a significant positive correlation between FA in the HD-tDCS group in the lATR and delayed memory subtest score changes (r = 0.76,

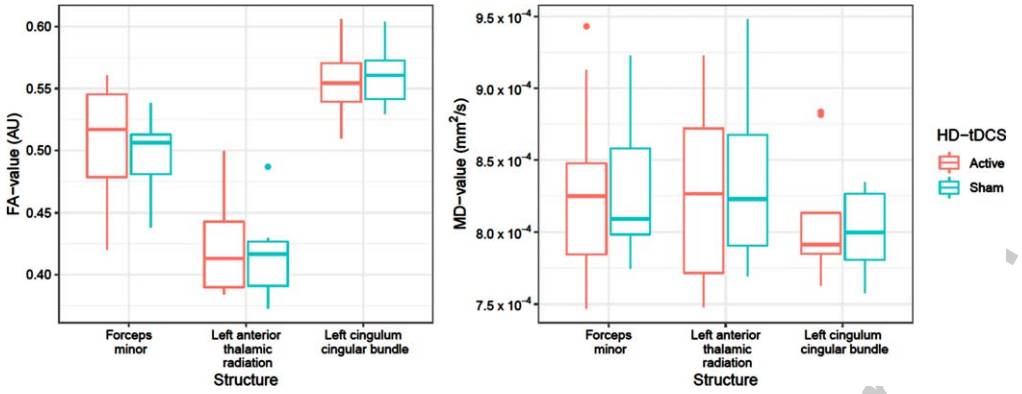

Fig. 8. Mean FA values (a) and mean MD values (b). Left anterior thalamic radiation (lATR); t(14) = 0.52, $p = 0.611$, left cingulum cingular bundle (lCCG); t(14) = –0.44, $p = 0.670$ and forceps minor (FMIN); t(14) = 0.37, $p = 0.721$ at baseline in the HD-tDCS and sham groups.

Table 4
Pearson correlations between delayed memory scores and DTI parameters in the HD-tDCS group

	1	2	3	4	5	6	7
1. *delayed memory SC*	1.000						
2. FA lATR	0.760*	1.000					
3. MD lATR	–0.290	–0.721	1.000				
4. FA lCCG	0.513	0.834**	–0.583	1.000			
5. MD lCCG	–0.524	–0.713*	466	–0.905**	1.000		
6. FA FMIN	–0.354	–0.468	0.459	–0.542	0.548	1.000	
7. MD FMIN	0.578	0.286	0.123	0.443	–0.498	–0.642	1.000

Delayed memory SC, delayed memory score change; lATR, left anterior thalamic radiation; lCCG, left cingulum cingular bundle; FMIN, forceps minor. *Significant at the 0.05 level, **significant at the 0.01 level. The tests are not *post hoc* corrected.

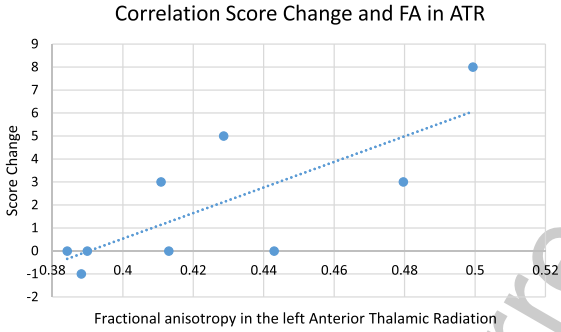

Fig. 9. Correlation of score change delayed memory and FA in the left Anterior Thalamic Radiation.

$p = 0.017$). The results are presented in a scatterplot (Fig. 9). There were no other significant results for FA or MD in the HD-tDCS group. In the sham group, there were no significant differences between changes in delayed memory performance and FA or MD.

DISCUSSION

The main purpose of this study was to investigate whether HD-tDCS leads to improvements in memory function in patients with AD. The second aim was to test relations between individual differences in brain anatomy and the cognitive effect of HD-tDCS. To increase the focality of tDCS, HD-tDCS was used, and electrode placement was individually optimized based on computational modeling of each participant's MRI scans.

Significant improvements in the primary outcome variable delayed memory and the secondary outcome variable MMSE were found in participants receiving HD-tDCS compared to the sham group. More specifically, five participants in the active group had higher scores on delayed memory post HD-tDCS, four remained stable and one declined with one point. The discovery of enhanced performance following tDCS is in line with previous findings in AD patients [63–65]. A review from Cai and colleagues, based on seven studies with a total of 146 AD patients concluded that tDCS had a significant effect on improving cognitive function overall; however, the results must be interpreted with caution. More specifically, considering previous studies on AD targeting the same region as the present study, the results regarding the therapeutic potential of tDCS vary. The conclusion of Boggio and colleagues [64] are in

accordance with our results, showing that tDCS over the left DLPFC had a positive effect on memory (measured with visual recognition tasks). Results from that study were based on a single 2 mA tDCS session, lasting for 30 min, compared to our accelerated design with a total of six 20 min sessions. Other studies that have shown improved cognitive performance after tDCS over the left DLPFC in AD patients have used MMSE scores as their measure of cognitive improvement; for example, the study by Khedr and colleagues [16] with 10 tDCS sessions and the home-based study by Im and colleagues [17] delivering 2 mA every day over a 6-month period. In contrast to our findings, Im et al. [16] did not find an improvement in delayed memory after tDCS. Delayed memory was not specifically measured by Khedr et al. [16]. Not all tDCS studies over the DLPFC have shown promising effects. The studies of Cotelli and colleagues [15] and Suemoto and colleagues [66] did not find tDCS superior to sham stimulation, measuring memory and apathy, respectively. Although the same target region was stimulated in all these studies, the primary outcome measures differ substantially. In addition, the severity of the disease at enrollment is inconsistent across studies. These factors make comparison of the studies challenging. As discussed by Khedr et al. [16], even though the electrode is placed over the DLPFC, the current prediction is uncertain. All previous studies have used conventional tDCS compared to the more focal HD-tDCS montage used in the present study. Since the current distributions vary in HD-tDCS and conventional tDCS electrode montages [31], comparisons between studies are problematic. Rather, our study should be considered as a proof-of principle study showing how HD-tDCS affects the E-field in the DLPFC of AD patients and exploring the relationship between HD-tDCS induced E-fields and cognitive measures.

A significant positive correlation between FA in the HD-tDCS group in the anterior thalamic radiation and the score change in the delayed memory subtest was found. These results support our hypothesis that participants with more intact white matter connections show stronger effects of HD-tDCS as a memory enhancer. The anterior thalamic nucleus receives information related to memory from the hippocampus, whereas the anterior thalamic radiation, a white matter bundle, connects the thalamus to the frontal cortex, especially to the DLPFC [23]. This result may indicate that patients with better-preserved white matter connections between the stimulation site and the thalamus/hippocampus benefitted the most from HD-tDCS. If this bundle is only moderately damaged, communication between the anterior thalamus and the left DLPFC may be enhanced by increasing DLPFC excitability, and thereby, the susceptibility of neurons in that region to inputs from the thalamus. In addition, the analysis of cortical thickness showed a tendency towards an association between larger thickness and score changes indicating improvement on the delayed memory subtest. Intriguingly, such associations were absent in the right hemisphere of patients receiving active HD-tDCS, or in both hemispheres of study participants in the sham HD-tDCS group. Those with more preserved gray and white matter connections may therefore be more susceptible to the beneficial effects of HD-tDCS. However, the relationship between cortical thickness and score changes was not significant, and the low sample size of 16 subjects in the DTI analysis must be taken into consideration when interpreting these results. The white matter tracts selected for the analysis was based on its structural closeness to the stimulated target (DLPFC), grounded in the hypothesis that structural connectivity between the stimulated target and the hippocampus influences tDCS effect. Another approach to study white matter as a predictor for tDCS effect is to target the fornix, which is memory-relevant tract with reduced FA values in AD patients. Adding this tract to the analysis could further explore if white matter alterations could guideline which patients are most likely to benefit from tDCS treatment.

The functional role of the HD-tDCS-induced E-field was studied by evaluating the relationship between the magnitude of the E-field normal component and score changes in delayed memory. Even though we found a large effect size in the net maximal anodal E-field in the DLPFC between participants in the HD-tDCS group that had positive score changes on the delayed memory subtest and participants in the HD-tDCS group with negative/no score changes, this finding was not significant. These results, though inconclusive, are in line with the findings of Kim and colleagues [34] in healthy participants. Mahdavi and colleagues' study demonstrated reduced current density in older adults with cognitive impairment compared to younger adults [30]. Antonenko and colleagues argued how the E-field variation between younger and older adults is affected by multiple factors, including atrophy, head anatomy, and brain state [67]. In the present study, we optimized electrode placement by analyzing E-field magnitude in the target are. However, we did not adjust the HD-tDCS

dose according to participants' head anatomy. Antenenko and colleagues demonstrated that the electric field is reduced in relation to head volume [67]. In future studies, computational modeling can be used to adjust the current intensity to different AD patients to ensure that a similar amount of E-field is induced in the region of interest across participants. Supporting this point of view, in a modeling study of healthy individuals, significant inter-individual variability in response to tDCS across a range of current intensities was observed [68].

In the present study we stimulated the left DLPFC. In AD, the DLPFC is hypothesized to be a compensatory brain resource, helping memory function when the function of the medial temporal lobes is reduced [14, 69, 70]. Gigi and colleagues argue that this compensatory mechanism is strongest in prodromal stages of AD and in mild stages of the disease, diminishing with severe AD [69]. This can be linked to our observation that patients with a thicker cortex and better white matter connections tended to improve more on delayed memory tasks than patients with a thinner cortex. Episodic memory depends on many higher cognitive functions, such as attention, recognition, and familiarity [71], and this merging is affected by the connectivity between structures [72]. The HD-tDCS group did also improve MMSE performance compared to the sham group. Nonetheless, MMSE is a non-specific screening measure of cognitive functioning, and cerebral correlates for this measure are global rather than focal [73]. In healthy controls, stimulation of the DLPFC improved consolidation of long-term memory, showing a lasting effect of tDCS. Several studies have focused on the prodromal phase and the therapeutic implications of DLPFC stimulation in patients with MCI rather than stimulating patients with developed AD [74].

The delayed memory subtest and the MMSE were the only scores that differed statistically between the HD-tDCS group and the sham group after the HD-tDCS intervention. The DLPFC is active both during working memory and attention tasks, and one would assume that these functions would also be affected by the anodal current in the targeted area. However, the effects of tDCS over the DLPFC on executive functions and attention are highly inconsistent, and face the same challenges as discussed above when comparing results due to different electrode montages and outcome measures [75]. Since attention was not improved in the HD-tDCS group, the improvement in delayed memory cannot be interpreted as a result of an increase in overall alertness. To further address the effect of tDCS on executive function in AD patients, specific executive tasks should be added to the test battery.

This study is the first to use HD-tDCS with the aim of improving memory impairment in AD patients. The results from our simulations resulted in four different HD-tDCS montages used to reach the maximal net anodal E-field in the left DLPFC. Considering the heterogeneity of cerebral atrophy in the AD population, focality in stimulation techniques is assumed to be especially important for reaching the desired region, considering that the current is affected by the CSF and the degree of atrophy [30]. Further analysis on a larger sample is needed to obtain more robust findings.

Based upon the literature up to September 2016, no recommendations could be made for the therapeutic approach of tDCS to enhance cognition in AD [76]. In recent years, several studies have explored different factors that can determine or affect the variations observed in the therapeutic response to tDCS, combining cognitive testing with biomarkers and neurophysiology [16, 17]. These combination studies provide information about the relationship between the cognitive effects observed after stimulation and the physiology behind tDCS. Even though the results at this point are scarce, exploratory studies are needed to establish clinical guidelines concerning the therapeutic potential of using tDCS in AD. Our study provides insights into how the HD-tDCS-induced E-field is distributed in the brain of an AD patient when using HD-tDCS over the left DLPFC. The significant results in our study, though on a small sample, support the need for further investigation of HD- tDCS as a therapeutic approach in AD.

The most substantial limitation of this study was the low sample size, which increased the risk of both type I and II errors. Unfortunately, low sample sizes are quite common in the AD-RCT field due to challenges in both recruitment and follow-up phases [77, 78]. In the present study a strict randomization procedure was followed, which resulted in significant baseline differences in delayed memory. There were also differences in patient characteristics of sex and age. Even though these differences were controlled for in the statistical analysis, this imbalance is a limitation to the study. In future studies, such biases could be reduced by using stratified randomization. In addition, we do not know if the significant improvement in delayed memory will persist over weeks or months. Another critical factor is that we did not apply a correction for multiple comparisons

to our cognitive tests. We opted not to correct for multiple comparisons to increase sensitivity to find potentially important effects (with the caveat of a higher risk for false positives, i.e., nonreplicable results). In this respect, our study should be regarded as proof-of-principle, and outcomes should be treated as preliminary.

None of the participants reported or showed signs of adverse effects. This is one of the benefits with tDCS. In addition, the devices are small, feasible and have a low cost. These advantages make it possible to consider tDCS as a treatment option for everyday use. Interesting home studies show promising results [17, 79]. Future studies should investigate the therapeutic effect of HD-tDCS on AD when combining daily sessions and optimized electrode positions.

In the present study an "offline" tDCS design was administrated. Whether online or offline stimulation is preferable is debatable, with studies on older adults showing in favor with offline designs [45, 80], while tDCS studies on other populations show "online" designs can give larger outcome effects on long- term memory [81]. Combining HD-tDCS with task relevant activity to AD patients may further increase tDCS effect since it potentiates task-relevant networks and should be further explored in future studies.

CONCLUSIONS

To increase focality in tDCS, computational modeling is a valuable method for analyzing the cortical flow of tDCS-induced E-field in AD. We found that HD-tDCS led to significantly improved delayed memory- and MMSE performance. Heterogeneity in brain anatomy resulted in four different montages when optimizing the electrode position to maximize the anodal intensity of DLPFC stimulation. FA in the lATR and score changes on the delayed memory subtest were positively correlated. Associations between the delayed memory effect of HD-tDCS and both E-field and cortical thickness were observed. These preliminary findings suggest that optimization of electrode placement may enhance the therapeutic effect of HD-tDCS as a memory enhancer in AD. Furthermore, patients with more preserved gray and white matter might benefit more from HD-tDCS than patients with more severe atrophy. tDCS therapy can be adjusted in the clinic to each patient's needs regarding brain anatomy, the degree of cortical atrophy and white matter alterations. A larger sample size is needed to draw firm conclusions.

ACKNOWLEDGMENTS

The research is funded by the Northern Norway Regional Health Authority (Helse Nord), with material support from UIT - The Arctic University of Norway.

Authors' disclosures available online (https://www.j-alz.com/manuscript-disclosures/21-0378r2).

SUPPLEMENTARY MATERIAL

The supplementary material is available in the electronic version of this article: http://dx.doi.org/10.3233/JAD-210378.

CLINICAL TRIAL REGISTRATION

www.ClinicalTrials.gov, Identifier: NCT03325205.

REFERENCES

[1] Andrieu S, Coley N, Lovestone S, Aisen PS, Vellas B (2015) Prevention of sporadic Alzheimer's disease: Lessons learned from clinical trials and future directions. *Lancet Neurol* **14**, 926-944.

[2] Cai M, Guo Z, Xing G, Peng H, Zhou L, Chen H, McClure MA, He L, Xiong L, He B, Du F, Mu Q (2019) Transcranial direct current stimulation improves cognitive function in mild to moderate Alzheimer disease: A meta-analysis. *Alzheimer Dis Assoc Disord* **33**, 170-178.

[3] Chang CH, Lane HY, Lin CH (2018) Brain stimulation in Alzheimer's disease. *Front Psychiatry* **9**, 201.

[4] Lam B, Masellis M, Freedman M, Stuss DT, Black SE (2013) Clinical, imaging, and pathological heterogeneity of the Alzheimer's disease syndrome. *Alzheimers Res Ther* **5**, 1.

[5] Opitz A, Paulus W, Will S, Antunes A, Thielscher A (2015) Determinants of the electric field during transcranial direct current stimulation. *Neuroimage* **109**, 140-150.

[6] Datta A, Truong D, Minhas P, Parra LC, Bikson M (2012) Inter-individual variation during transcranial direct current stimulation and normalization of dose using MRI-derived computational models. *Front Psychiatry* **3**, 91.

[7] Bäckman L, Jones S, Berger AK, Laukka EJ, Small BJ (2005) Cognitive impairment in preclinical Alzheimer's disease: A meta-analysis. *Neuropsychology* **19**, 520-531.

[8] Weston PSJ, Nicholas JM, Henley SMD, Liang Y, Macpherson K, Donnachie E, Schott JM, Rossor MN, Crutch SJ, Butler CR, Zeman AZ, Fox NC (2018) Accelerated long-term forgetting in presymptomatic autosomal dominant Alzheimer's disease: A cross-sectional study. *Lancet Neurol* **17**, 123-132.

[9] Weissberger GH, Strong JV, Stefanidis KB, Summers MJ, Bondi MW, Stricker NH (2017) Diagnostic accuracy of memory measures in Alzheimer's dementia and mild cognitive impairment: A systematic review and meta-analysis. *Neuropsychol Rev* **27**, 354-388.

[10] Frisoni GB, Fox NC, Jack CR, Jr., Scheltens P, Thompson PM (2010) The clinical use of structural MRI in Alzheimer disease. *Nat Rev Neurol* **6**, 67-77.

[11] Vemuri P, Jack CR, Jr. (2010) Role of structural MRI in Alzheimer's disease. *Alzheimers Res Ther* **2**, 23.

[12] Whitwell JL, Przybelski SA, Weigand SD, Knopman DS, Boeve BF, Petersen RC, Jack CR, Jr. (2007) 3D maps from multiple MRI illustrate changing atrophy patterns as subjects progress from mild cognitive impairment to Alzheimer's disease. *Brain* **130**, 1777-1786.

[13] Perry RJ, Hodges JR (1999) Attention and executive deficits in Alzheimer's disease. A critical review. *Brain* **122 (Pt 3)**, 383-404.

[14] Kumar S, Zomorrodi R, Ghazala Z, Goodman MS, Blumberger DM, Cheam A, Fischer C, Daskalakis ZJ, Mulsant BH, Pollock BG, Rajji TK (2017) Extent of dorsolateral prefrontal cortex plasticity and its association with working memory in patients with Alzheimer disease. *JAMA Psychiatry* **74**, 1266-1274.

[15] Cotelli M, Manenti R, Brambilla M, Petesi M, Rosini S, Ferrari C, Zanetti O, Miniussi C (2014) Anodal tDCS during face-name associations memory training in Alzheimer's patients. *Front Aging Neurosci* **6**, 38.

[16] Khedr EM, Gamal NF, El-Fetoh NA, Khalifa H, Ahmed EM, Ali AM, Noaman M, El-Baki AA, Karim AA (2014) A double-blind randomized clinical trial on the efficacy of cortical direct current stimulation for the treatment of Alzheimer's disease. *Front Aging Neurosci* **6**, 275.

[17] Im JJ, Jeong H, Bikson M, Woods AJ, Unal G, Oh JK, Na S, Park JS, Knotkova H, Song IU, Chung YA (2019) Effects of 6-month at-home transcranial direct current stimulation on cognition and cerebral glucose metabolism in Alzheimer's disease. *Brain Stimul* **12**, 1222-1228.

[18] Liu CS, Herrmann N, Gallagher D, Rajji TK, Kiss A, Vieira D, Lanctôt KL (2020) A pilot study comparing effects of bifrontal versus bitemporal transcranial direct current stimulation in mild cognitive impairment and mild Alzheimer disease. *J ECT* **36**, 211-215.

[19] Kuo HI, Paulus W, Batsikadze G, Jamil A, Kuo MF, Nitsche MA (2016) Chronic enhancement of serotonin facilitates excitatory transcranial direct current stimulation-induced neuroplasticity. *Neuropsychopharmacology* **41**, 1223-1230.

[20] Sachdev PS, Zhuang L, Braidy N, Wen W (2013) Is Alzheimer's a disease of the white matter? *Curr Opin Psychiatry* **26**, 244-251.

[21] Oishi K, Mielke MM, Albert M, Lyketsos CG, Mori S (2011) DTI analyses and clinical applications in Alzheimer's disease. *J Alzheimers Dis* **26 Suppl 3**, 287-296.

[22] Lee SH, Coutu JP, Wilkens P, Yendiki A, Rosas HD, Salat DH (2015) Tract-based analysis of white matter degeneration in Alzheimer's disease. *Neuroscience* **301**, 79-89.

[23] Niida R, Yamagata B, Niida A, Uechi A, Matsuda H, Mimura M (2018) Aberrant anterior thalamic radiation structure in bipolar disorder: A diffusion tensor tractography study. *Front Psychiatry* **9**, 522.

[24] George K, Das JM (2020) Neuroanatomy, thalamocortical radiations. In *StatPearls.* StatPearls Publishing, Treasure Island (FL).

[25] Chua TC, Wen W, Slavin MJ, Sachdev PS (2008) Diffusion tensor imaging in mild cognitive impairment and Alzheimer's disease: A review. *Curr Opin Neurol* **21**, 83-92.

[26] Zhao H, Qiao L, Fan D, Zhang S, Turel O, Li Y, Li J, Xue G, Chen A, He Q (2017) Modulation of brain activity with noninvasive transcranial direct current stimulation (tDCS): Clinical applications and safety concerns. *Front Psychol* **8**, 685.

[27] Li LM, Violante IR, Leech R, Hampshire A, Opitz A, McArthur D, Carmichael DW, Sharp DJ (2019) Cognitive enhancement with salience network electrical stimulation is influenced by network structural connectivity. *Neuroimage* **185**, 425-433.

[28] Miranda PC, Lomarev M, Hallett M (2006) Modeling the current distribution during transcranial direct current stimulation. *Clin Neurophysiol* **117**, 1623-1629.

[29] Mahdavi S, Yavari F, Gharibzadeh S, Towhidkhah F (2014) Modeling studies for designing transcranial direct current stimulation protocol in Alzheimer's disease. *Front Comput Neurosci* **8**, 72.

[30] Mahdavi S, Towhidkhah F (2018) Computational human head models of tDCS: Influence of brain atrophy on current density distribution. *Brain Stimul* **11**, 104-107.

[31] Bikson M, Rahman A, Datta A, Fregni F, Merabet L (2012) High-resolution modeling assisted design of customized and individualized transcranial direct current stimulation protocols. *Neuromodulation* **15**, 306-315.

[32] Neuling T, Wagner S, Wolters CH, Zaehle T, Herrmann CS (2012) Finite-element model predicts current density distribution for clinical applications of tDCS and tACS. *Front Psychiatry* **3**, 83.

[33] Dmochowski JP, Datta A, Bikson M, Su Y, Parra LC (2011) Optimized multi-electrode stimulation increases focality and intensity at target. *J Neural Eng* **8**, 046011.

[34] Csifcsák G, Boayue NM, Puonti O, Thielscher A, Mittner M (2018) Effects of transcranial direct current stimulation for treating depression: A modeling study. *J Affect Disord* **234**, 164-173.

[35] Edwards D, Cortes M, Datta A, Minhas P, Wassermann EM, Bikson M (2013) Physiological and modeling evidence for focal transcranial electrical brain stimulation in humans: A basis for high-definition tDCS. *Neuroimage* **74**, 266-275.

[36] Kim JH, Kim DW, Chang WH, Kim YH, Im CH (2013) Inconsistent outcomes of transcranial direct current stimulation (tDCS) may be originated from the anatomical differences among individuals: A simulation study using individual MRI data. *Annu Int Conf IEEE Eng Med Biol Soc* **2013**, 823-825.

[37] McKhann G, Drachman D, Folstein M, Katzman R, Price D, Stadlan EM (1984) Clinical diagnosis of Alzheimer's disease: Report of the NINCDS-ADRDA Work Group under the auspices of Department of Health and Human Services Task Force on Alzheimer's Disease. *Neurology* **34**, 939-944.

[38] McKhann GM, Knopman DS, Chertkow H, Hyman BT, Jack CR, Jr., Kawas CH, Klunk WE, Koroshetz WJ, Manly JJ, Mayeux R, Mohs RC, Morris JC, Rossor MN, Scheltens P, Carrillo MC, Thies B, Weintraub S, Phelps CH (2011) The diagnosis of dementia due to Alzheimer's disease: Recommendations from the National Institute on Aging-Alzheimer's Association workgroups on diagnostic guidelines for Alzheimer's disease. *Alzheimers Dement* **7**, 263-269.

[39] Saturnino GB, Puonti O, Nielsen JD, Antonenko D, Madsen KH, Thielscher A (2019) SimNIBS 2.1: A comprehensive pipeline for individualized electric field modelling for transcranial brain stimulation. In *Brain and Human Body Modeling: Computational Human Modeling at EMBC 2018*, Makarov S, Horner M, Noetscher G, eds. Springer-Copyright 2019, Cham, pp. 3-25.

[40] Saturnino GB, Antunes A, Thielscher A (2015) On the importance of electrode parameters for shaping electric field patterns generated by tDCS. *Neuroimage* **120**, 25-35.

[41] Rahman A, Lafon B, Parra LC, Bikson M (2017) Direct current stimulation boosts synaptic gain and cooperativity *in vitro*. *J Physiol* **595**, 3535-3547.

[42] Ranta ME, Chen M, Crocetti D, Prince JL, Subramaniam K, Fischl B, Kaufmann WE, Mostofsky SH (2014) Automated MRI parcellation of the frontal lobe. *Hum Brain Mapp* **35**, 2009-2026.

[43] Ranta ME, Crocetti D, Clauss JA, Kraut MA, Mostofsky SH, Kaufmann WE (2009) Manual MRI parcellation of the frontal lobe. *Psychiatry Res* **172**, 147-154.

[44] Huang Y, Dmochowski JP, Su Y, Datta A, Rorden C, Parra LC (2013) Automated MRI segmentation for individualized modeling of current flow in the human head. *J Neural Eng* **10**, 066004.

[45] Summers JJ, Kang N, Cauraugh JH (2016) Does transcranial direct current stimulation enhance cognitive and motor functions in the ageing brain? A systematic review and meta-analysis. *Ageing Res Rev* **25**, 42-54.

[46] Monte-Silva K, Kuo MF, Hessenthaler S, Fresnoza S, Liebetanz D, Paulus W, Nitsche MA (2013) Induction of late LTP-like plasticity in the human motor cortex by repeated non-invasive brain stimulation. *Brain Stimul* **6**, 424-432.

[47] Randolph C, Tierney MC, Mohr E, Chase TN (1998) The Repeatable Battery for the Assessment of Neuropsychological Status (RBANS): Preliminary clinical validity. *J Clin Exp Neuropsychol* **20**, 310-319.

[48] Schmitt AL, Livingston RB, Goette WF, Galusha-Glasscock JM (2016) Relationship between the Mini-Mental State Examination and the Repeatable Battery for the Assessment of Neuropsychological Status in patients referred for a dementia evaluation. *Percept Mot Skills* **123**, 606-623.

[49] Garcia C, Leahy B, Corradi K, Forchetti C (2008) Component structure of the Repeatable Battery for the Assessment of Neuropsychological Status in dementia. *Arch Clin Neuropsychol* **23**, 63-72.

[50] Duff K, Humphreys Clark JD, O'Bryant SE, Mold JW, Schiffer RB, Sutker PB (2008) Utility of the RBANS in detecting cognitive impairment associated with Alzheimer's disease: Sensitivity, specificity, and positive and negative predictive powers. *Arch Clin Neuropsychol* **23**, 603-612.

[51] Folstein MF, Folstein SE, McHugh PR (1975) Mini-mental state: A practical method for grading the cognitive state of patients for the clinician. *J Psychiatr Res* **12**, 189-198.

[52] Shulman KI (2000) Clock-drawing: Is it the ideal cognitive screening test? *Int J Geriatr Psychiatry* **15**, 548-561.

[53] Tombaugh TN (2004) Trail Making Test A and B: Normative data stratified by age and education. *Arch Clin Neuropsychol* **19**, 203-214.

[54] Fischl B (2012) FreeSurfer. *Neuroimage* **62**, 774-781.

[55] Fischl B, Dale AM (2000) Measuring the thickness of the human cerebral cortex from magnetic resonance images. *Proc Natl Acad Sci U S A* **97**, 11050-11055.

[56] Fischl B, Salat DH, Busa E, Albert M, Dieterich M, Haselgrove C, van der Kouwe A, Killiany R, Kennedy D, Klaveness S, Montillo A, Makris N, Rosen B, Dale AM (2002) Whole brain segmentation: Automated labeling of neuroanatomical structures in the human brain. *Neuron* **33**, 341-355.

[57] Fischl B, van der Kouwe A, Destrieux C, Halgren E, Ségonne F, Salat DH, Busa E, Seidman LJ, Goldstein J, Kennedy D, Caviness V, Makris N, Rosen B, Dale AM (2004) Automatically parcellating the human cerebral cortex. *Cereb Cortex* **14**, 11-22.

[58] Winkler AM, Ridgway GR, Webster MA, Smith SM, Nichols TE (2014) Permutation inference for the general linear model. *Neuroimage* **92**, 381-397.

[59] Smith SM, Nichols TE (2009) Threshold-free cluster enhancement: Addressing problems of smoothing, threshold dependence and localisation in cluster inference. *Neuroimage* **44**, 83-98.

[60] Winkler AM, Ridgway GR, Douaud G, Nichols TE, Smith SM (2016) Faster permutation inference in brain imaging. *Neuroimage* **141**, 502-516.

[61] Yendiki A, Panneck P, Srinivasan P, Stevens A, Zöllei L, Augustinack J, Wang R, Salat D, Ehrlich S, Behrens T, Jbabdi S, Gollub R, Fischl B (2011) Automated probabilistic reconstruction of white-matter pathways in health and disease using an atlas of the underlying anatomy. *Front Neuroinform* **5**, 23.

[62] Wakana S, Caprihan A, Panzenboeck MM, Fallon JH, Perry M, Gollub RL, Hua K, Zhang J, Jiang H, Dubey P, Blitz A, van Zijl P, Mori S (2007) Reproducibility of quantitative tractography methods applied to cerebral white matter. *Neuroimage* **36**, 630-644.

[63] Boggio PS, Khoury LP, Martins DC, Martins OE, de Macedo EC, Fregni F (2009) Temporal cortex direct current stimulation enhances performance on a visual recognition memory task in Alzheimer disease. *J Neurol Neurosurg Psychiatry* **80**, 444-447.

[64] Boggio PS, Ferrucci R, Mameli F, Martins D, Martins O, Vergari M, Tadini L, Scarpini E, Fregni F, Priori A (2012) Prolonged visual memory enhancement after direct current stimulation in Alzheimer's disease. *Brain Stimul* **5**, 223-230.

[65] Ferrucci R, Mameli F, Guidi I, Mrakic-Sposta S, Vergari M, Marceglia S, Cogiamanian F, Barbieri S, Scarpini E, Priori A (2008) Transcranial direct current stimulation improves recognition memory in Alzheimer disease. *Neurology* **71**, 493-498.

[66] Suemoto CK, Apolinario D, Nakamura-Palacios EM, Lopes L, Leite RE, Sales MC, Nitrini R, Brucki SM, Morillo LS, Magaldi RM, Fregni F (2014) Effects of a non-focal plasticity protocol on apathy in moderate Alzheimer's disease: A randomized, double-blind, sham-controlled trial. *Brain Stimul* **7**, 308-313.

[67] Antonenko D, Grittner U, Saturnino G, Nierhaus T, Thielscher A, Flöel A (2020) Inter-individual and age-dependent variability in simulated electric fields induced by conventional transcranial electrical stimulation. *Neuroimage* **224**, 117413.

[68] Chew T, Ho KA, Loo CK (2015) Inter- and intra-individual variability in response to transcranial direct current stimulation (tDCS) at varying current intensities. *Brain Stimul* **8**, 1130-1137.

[69] Gigi A, Babai R, Penker A, Hendler T, Korczyn AD (2010) Prefrontal compensatory mechanism may enable normal semantic memory performance in mild cognitive impairment (MCI). *J Neuroimaging* **20**, 163-168.

[70] Becker JT, Mintun MA, Aleva K, Wiseman MB, Nichols T, DeKosky ST (1996) Compensatory reallocation of brain resources supporting verbal episodic memory in Alzheimer's disease. *Neurology* **46**, 692-700.

[71] Cabeza R (2008) Role of parietal regions in episodic memory retrieval: The dual attentional processes hypothesis. *Neuropsychologia* **46**, 1813-1827.

[72] Reid AT, Evans AC (2013) Structural networks in Alzheimer's disease. *Eur Neuropsychopharmacol***23**, 63-77.

[73] Fjell AM, Amlien IK, Westlye LT, Walhovd KB (2009) Mini-mental state examination is sensitive to brain atrophy in Alzheimer's disease. *Dement Geriatr Cogn Disord* **28**, 252-258.

[74] Meinzer M, Lindenberg R, Phan MT, Ulm L, Volk C, Flöel A (2015) Transcranial direct current stimulation in mild cognitive impairment: Behavioral effects and neural mechanisms. *Alzheimers Dement* **11**, 1032-1040.

[75] Tremblay S, Lepage JF, Latulipe-Loiselle A, Fregni F, Pascual-Leone A, Théoret H (2014) The uncertain outcome of prefrontal tDCS. *Brain Stimul* **7**, 773-783.

[76] Lefaucheur JP, Antal A, Ayache SS, Benninger DH, Brunelin J, Cogiamanian F, Cotelli M, De Ridder D, Ferrucci R, Langguth B, Marangolo P, Mylius V, Nitsche MA, Padberg F, Palm U, Poulet E, Priori A, Rossi S, Schecklmann M, Vanneste S, Ziemann U, Garcia-Larrea L, Paulus W (2017) Evidence-based guidelines on the therapeutic use of transcranial direct current stimulation (tDCS). *Clin Neurophysiol* **128**, 56-92.

[77] Clement C, Selman LE, Kehoe PG, Howden B, Lane JA, Horwood J (2019) Challenges to and facilitators of recruitment to an Alzheimer's disease clinical trial: A qualitative interview study. *J Alzheimers Dis* **69**, 1067-1075.

[78] Grill JD, Karlawish J (2010) Addressing the challenges to successful recruitment and retention in Alzheimer's disease clinical trials. *Alzheimers Res Ther* **2**, 34.

[79] Bystad M, Rasmussen ID, Grønli O, Aslaksen PM (2017) Can 8 months of daily tDCS application slow the cognitive decline in Alzheimer's disease? A case study. *Neurocase* **23**, 146-148.

[80] Indahlastari A, Hardcastle C, Albizu A, Alvarez-Alvarado S, Boutzoukas EM, Evangelista ND, Hausman HK, Kraft J, Langer K, Woods AJ (2021) A systematic review and meta-analysis of transcranial direct current stimulation to remediate age-related cognitive decline in healthy older adults. *Neuropsychiatr Dis Treat* **17**, 971-990.

[81] Au J, Karsten C, Buschkuehl M, Jaeggi SM (2017) Optimizing transcranial direct current stimulation protocols to promote long-term learning. *J Cogn Enhance* **1**, 65-72.